JOURNAL OF GEOPHYSICAL RESEARCH, VOL. 112, D23103, doi:10.1029/2006JD007673, 2007

Stratospheric transport using 6-h-averaged winds from a data assimilation system

Steven Pawson,[1] Ivanka Stajner,[1,2] S. Randolph Kawa,[3] Hiroo Hayashi,[1,4] Wei-Wu Tan,[1,2] J. Eric Nielsen,[1,5] Zhengxin Zhu,[3,5] Lang-Ping Chang,[1,2] and Nathaniel J. Livesey[6]

Received 19 June 2006; revised 17 April 2007; accepted 10 August 2007; published 8 December 2007.

[1] Stratospheric transport calculated using assimilated winds has been shown to be too fast in many cases, because of excessive mixing and an overstrong residual circulation. It is shown that the use of 6-h-averaged wind fields instead of instantaneous analyses can substantially reduce this problem for NASA's Goddard Earth Observing System version 4 (GEOS-4) sequential data assimilation system. Two examples are used to illustrate impacts in an off-line chemistry transport model. An age-of-air computation shows that the stratosphere becomes substantially older when time-averaged winds are used, yet still not as old as that determined from observations. An ozone assimilation experiment reveals improvements in the spatial structure of assimilated ozone, better agreement with independent observations, and a 40–60% reduction in observation-minus-forecast residuals. The averaged meteorological fields have also been incorporated in the on-line transport computations: This is equivalent to using a 6-h square-wave filter at the analysis times. Sub-6-h noise in the system is substantially reduced with this approach. Two additional examples of transport are shown. A simulation of 2004–2005 shows that the descent of N_2O in the Arctic polar vortex is represented more accurately than in previous studies. A tape recorder signal is evident in the tropical moisture; it ascends about 30% faster than that in the real atmosphere. In summary, the use of 6-h-averaged winds substantially improves the transport characteristics of the assimilated data, although the circulation remains too fast.

Citation: Pawson, S., I. Stajner, S. R. Kawa, H. Hayashi, W.-W. Tan, J. E. Nielsen, Z. Zhu, L.-P. Chang, and N. J. Livesey (2007), Stratospheric transport using 6-h-averaged winds from a data assimilation system, *J. Geophys. Res.*, *112*, D23103, doi:10.1029/2006JD007673.

1. Introduction

[2] Dynamics and transport play a central role in stratospheric chemistry. An example is the importance of confinement of air masses inside the polar vortex for the formation of the ozone hole. For evaluation and process understanding, statistical properties of chemical distributions can be understood using free-running general circulation models (GCMs) [e.g., *Sankey and Shepherd*, 2003]. However, detailed studies of atmospheric chemistry data obtained in specific events require transport computations using winds from those times, as can be obtained through data assimilation [e.g., *Rood et al.*, 1991]. Accurate wind analyses are thus needed to interpret space-based constituent data using chemistry-transport models (CTMs) as interpretative tools. One such example is the understanding of features in trace gas distributions, such as modeling the origin of ozone filaments detected by the Earth-Observation System Microwave Limb Sounder (EOS MLS) instrument and a ground-based lidar in Hawaii [*Leblanc et al.*, 2006]. Another example is for simulations of interannual variations in ozone, modeled with a CTM by *Hadjinicolaou et al.* [2002]. These studies used CTMs driven by analyzed winds from different versions of the analysis system from the European Centre for Medium-Range Weather Forecasts (ECMWF).

[3] The accuracy of transport computations using analyzed winds is questionable. While rapid, quasi-horizontal features in trace gas distributions can be captured [*Rood et al.*, 1991; *Leblanc et al.*, 2006], the slowly varying features of the flow are often not well represented because of an overstrong residual circulation [e.g., *Weaver et al.*, 1993; *Meijer et al.*, 2004] and excessive mixing [e.g., *Schoeberl et al.*, 2003; *Tan et al.*, 2004]. This anomalous transport has important consequences. Using a CTM driven by Goddard Earth Observing System, version 3 (GEOS-3) analyses, *Considine et al.* [2003] found that polar chemistry was

[1]Global Modeling and Assimilation Office, NASA Goddard Space Flight Center, Greenbelt, Maryland, USA.
[2]Science Applications International Corporation, Beltsville, Maryland, USA.
[3]Atmospheric Chemistry and Dynamics Branch, NASA Goddard Space Flight Center, Greenbelt, Maryland, USA.
[4]Goddard Earth Sciences and Technology Center, University of Maryland, Baltimore, Maryland, USA.
[5]Science Systems and Applications Inc., Lanham, Maryland, USA.
[6]Jet Propulsion Laboratory, Pasadena, California, USA.

0148-0227/07/2006JD007673$09.00

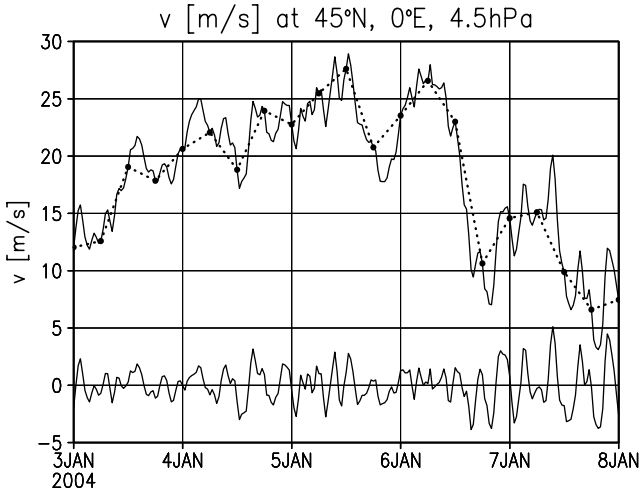

Figure 1. The meridional velocity (m/s) at 0°E and 45°N, between 00Z 3 January 2004 and 00Z 8 January 2004. The solid circles show the analysis times every 6 h and are connected with the dashed lines (the linear fit between the analyses). The solid curve passing through the analyses shows the velocity archived at 30-min intervals. The lower solid curve shows the same data with the 6-h running mean subtracted, qualitatively emphasizing the sub-6-hourly variability.

inadequately represented because of excessive mixing in and around the Arctic polar vortex in 2001. In an ozone assimilation system using GEOS-4 winds, biases from transport errors could be corrected using a higher density of ozone data [*Wargan et al.*, 2005].

[4] Similar transport problems have been identified in many meteorological analyses, including those from ECMWF [*Stöhl et al.*, 2004; *van Noije et al.*, 2004], the Met. Office of the United Kingdom [*Schoeberl et al.*, 2003], and GEOS-4 [*Schoeberl et al.*, 2003; *Tan et al.*, 2004]. In recent ECMWF analyses, where one change is an update from three- to four-dimensional variational (3D- to 4D-Var) assimilation, the problem is reduced [*Meijer et al.*, 2004; *Scheele et al.*, 2005]. While there is optimism that data assimilation techniques may eventually be developed that eliminate the problem, or at least reduce its magnitude, other methods must presently be adopted when using meteorological analyses for atmospheric chemistry studies.

[5] One approach, based on medium-range forecasts rather than analyses, has been exploited. Following *Wild et al.* [2003], who used ECMWF forecasts to drive a tropospheric CTM, *Meijer et al.* [2004] demonstrated that use of 1- or 3-d forecasts substantially increased the age of air (AA) in stratospheric computations. However, even in the best case (3-d forecasts initialized with 4D-Var analyses) the AA remained about 1–1.5 years (a) lower than that inferred from observations. Despite the improved AA simulation, the general benefit of using forecast winds remains to be demonstrated; temporal growth in forecast error may limit the applicability in situations when spatial variability in transport impacts the field of interest, such as constituent assimilation.

[6] The present study demonstrates that the alternate approach of using time averages of the meteorological fields also reduces the transport problems. *Waugh et al.* [1997] demonstrated that transport in a CTM driven by winds from a GCM was substantially better when 3-h averages were used in place of instantaneous values. This is because the subsampling at discrete times led to aliasing problems, while the time-averaging filtered the transient components and reduced spurious transport. This study uses 6-h-averaged fields, as explained in section 2. Results are presented for different problems in off-line (sections 3 and 4) and on-line (section 5) frameworks. Section 6 summarizes the main results and discusses their possible generality.

2. GEOS-4 Assimilation System and Motivation for Time Averaging

[7] The GEOS-4.0.3 data assimilation system [*Bloom et al.*, 2005] was used in this work; *Tan et al.* [2004] used an earlier version (4.0.2) of this system. GEOS-4 is based on the Physical-Space Statistical Analysis Scheme [*Cohn et al.*, 1998], a form of 3D-Var in which the optimization is performed at observation locations, rather than on the model grid. The underlying GCM is based on the dynamical core of *Lin* [2004] and the physical parameterizations of *Kiehl et al.* [1998]. A wide range of data is ingested, of which winds from radiosondes and thermal structure from radiosondes and the Advanced Microwave Sounding Unit (AMSU) are the most relevant for the middle atmosphere [*Bloom et al.*, 2005]. The sequential assimilation is performed in a 6-h cycle, producing analyses at the synoptic times of 00, 06, 12 and 18 UT. The assimilation combines background fields (6-h forecasts from the previous analyses) with all available data from within a 6-h window centered on the synoptic times.

[8] In the development and validation of GEOS-4, substantial high-frequency variance was isolated. For illustration, Figure 1 shows a 5-d (3–8 January 2004) time series of meridional velocity (v) plotted at 30-min intervals at a representative point (0°E, 45°N, 4.5 hPa). While a range of frequencies is evident in the time series, there is a substantial contribution of the 6-h wave, which is emphasized by subtracting the 6-h running mean. Note that many of the sharpest changes in Figure 1 do not coincide with analysis times. Data withholding experiments reveal that much of the noisiness originates primarily through data insertion in the troposphere and propagates upward, growing as density decreases in the middle atmosphere. These oscillations in GEOS-4.0.3 are stronger than in GEOS-4.0.2 used by *Tan et al.* [2004]; one important factor in this is that greater weight is given to the observations in the present system. The "finite-volume data assimilation system" used by *Schoeberl et al.* [2003] and *Douglass et al.* [2003] was an early test version of GEOS-4 that gave data a very low weight and used a different version of the GCM; it also had a smoother temporal behavior.

[9] Meteorological analyses typically archive snapshots every 6 h, shown by the solid circles in Figure 1, leading to an aliasing of the sub-6-hourly variability (compare the solid and dashed lines) that is used in CTMs. These oscillations appear as spatiotemporal patterns in fields such as horizontal divergence and vertical velocity, with reversals in the patterns through any 6-h period. This leads to superfluous spatial mixing, which is enhanced in off-line

computations because of aliasing when only 6-hourly samples are available.

[10] The importance of temporal sampling has been addressed in prior studies. *Waugh et al.* [1997] showed that aliasing of transience led to inaccuracies in CTM transport driven by archived fields from a GCM. Introducing 3-h averages substantially improved the transport calculations. When using analyses, the additional "shock" caused by data insertion can make the problem more acute. *Legras et al.* [2005] generated time-smoothed fields at 3-hourly intervals from ECMWF data in their trajectory model-data study of turbulent diffusion in the lower stratosphere. The smoothing was shown to be essential for realistic trace-gas simulations. The time smoothing was performed using 6-hourly analyses (for 0, 6, 12, and 18 UT) along with forecasts at the intermediate 3-hourly intervals (at 3, 9, 15, and 21 UT). Similar conclusions about the use of such 3-h sampling were made by *Berthet et al.* [2006] and by *Bregman et al.* [2006] in their CTM studies.

[11] A different approach is adopted in this study: The 6-h averages of the meteorological fields are computed as the GEOS-4 system runs. This is equivalent to using a square-wave filter. The filtering properties of this time averaging are well known [e.g., *Press et al.*, 1992]: Advantages are that the 6-, 3-, and 2-h components of variability are entirely eliminated from the data, while a potential disadvantage is that the semidiurnal and diurnal components are suppressed. *Swinbank et al.* [1999] demonstrated inaccurately represented tides in the upper stratosphere of the GEOS-2 data assimilation system. The problem was partly related to the 6-h data windows, which are unchanged in GEOS-4. Given the uncertainty in representing these tides, they have been given low priority here. This study presents the case for using the 6-h average, demonstrating credible aspects of using time-averaged GEOS-4 data in transport computations.

3. Impacts on Age of Air

[12] In this section, computations of age-of-air (AA) [*Hall and Plumb*, 1994] using a CTM are shown. The CTM used in this work is based on the flux-form semi-Lagrangian transport code of *Lin and Rood* [1996]. All experiments described here used a spatial resolution of 2.5° (longitude) × 2° (latitude). The CTM uses meteorological fields from the GEOS-4 analyses, including winds, temperature, and quantities such as cloud-mass fluxes that drive the "sub-grid-scale" transport. The CTM can use chemistry modules of varying complexity, ranging from passive species such as SF_6 [*Schoeberl et al.*, 2003], through linearized chemical production and loss rates [*Stajner et al.*, 2004], to full chemical mechanisms [*Douglass et al.*, 2003]. The experiments in this section use the CTM constrained by 6-hourly archives of either "instantaneous" or "6-h-averaged" winds and temperatures from the GEOS-4 analyses; the fields are linearly interpolated in time to the model time step of 30 min.

[13] AA [*Hall and Plumb*, 1994] is a measure of the time that an air mass has remained in the stratosphere since entering through the tropical tropopause. The mean AA can be computed using long-lived trace gases with linearly increasing source gas (e.g., SF_6), while the spectrum can be computed using pulsed releases of inert tracers. The mean age and the age spectrum are established diagnostics for quantifying the strengths of the Brewer-Dobson circulation and meridional mixing on stratospheric transport [e.g., *Schoeberl et al.*, 2003]. The mean AA deduced from observations is 4–5 a near 50 hPa in the polar stratosphere [*Andrews et al.*, 2001]. An overintense Brewer-Dobson circulation leads to an underestimate of mean age. Excessive meridional mixing between the tropics and polar regions reduces meridional gradients and broadens the age spectrum. Studies with various assimilated data sets have revealed a tendency to underestimate age, display weak meridional gradients and a broad AA spectrum [*Schoeberl et al.*, 2003; *Meijer et al.*, 2004]. AA characteristics using assimilated data sets are worse than those computed from free-running GCMs [*Douglass et al.*, 2003; *Schoeberl et al.*, 2003] because of the additional mixing introduced by the data insertion [*Tan et al.*, 2004].

[14] These same characteristics are evident in GEOS-4 (Figure 2, left): The mean AA at 50 hPa near the Pole barely exceeds 1 a and meridional gradients are very weak. This computation was performed using the CTM with an SF_6 tracer constrained to equal model time at the surface, with an upper boundary at 0.2 hPa. The mean AA is normalized be zero at 100 hPa at the equator. A comparable calculation with 6-h-averaged winds shows the following improvements in mean AA (Figure 2, right): (1) a more prominent tropical pipe, (2) AA values approaching 4 a in the upper stratosphere, and (3) extension of the 3.25/3.5-a contours down to 50 hPa at the North/South Poles. These results show that the transport with the 6-h-averaged winds is much slower and more realistic than that with instantaneous winds. Differences in the troposphere are caused by more rapid transport across the tropopause with instantaneous winds.

[15] An experiment using pulsed releases in the troposphere was performed to compute the age spectra using both time-averaged and instantaneous winds in the CTM. The results (Figure 3) show spectra at 50 hPa of similar shapes in the Tropics and with rather larger spread in northern middle latitudes. The tropical spectra both display a sharp peak at young ages, indicating the more rapid vertical transport with instantaneous winds (the mode is six months younger) and the more rapid recirculation, with a tail decaying by 5 a when instantaneous winds are used but retaining a small fraction of ages up to about 9 a when 6-h averages are used. At 60°N, the spectra at 50 hPa exhibit larger differences, peaking (with a hint of bimodality) at 10–12 months when instantaneous winds are used but near 2 a when 6-h averages are used. These features illustrate the excessive vertical transport throughout the atmosphere when instantaneous wind fields are used, but a much more realistic depiction of transport with 6-h-averaged winds.

[16] These improvements are similar to those obtained by *Meijer et al.* [2004]. Using ECMWF analyses, their computed AA near 50 hPa in the polar region was 1.5–2 a using 3D-Var and 2.5–3 a using 4D-Var analyses, with the younger ages in the northern hemisphere. AA increased to almost 3.5 a when 3-d forecast winds from the 4D-Var system were used in the CTM. The AA computed using the 6-h-averaged GEOS-4 winds is comparable to the best case presented by *Meijer et al.* [2004]. (The use of different

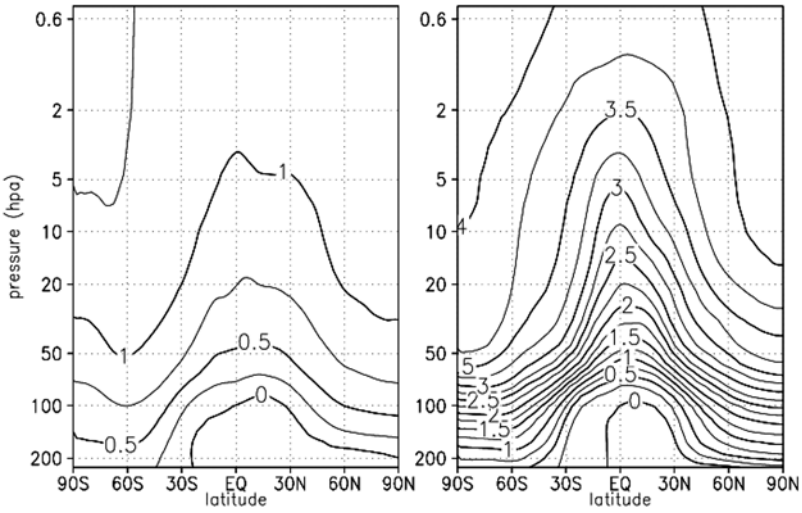

Figure 2. The age of air (AA) computed from the Goddard Earth Observing System version 4 (GEOS-4) assimilation system using 4-times-daily winds. Results are shown for (left) instantaneous output and (right) 6-h mean output. Contour interval is 0.25 a.

CTMs may impact this result, in addition to the impact of different analyses.)

[17] In summary, the AA is substantially increased by the 6-h averaging, but it remains younger than that inferred from atmospheric observations, which is about 4–5 a in the polar lower stratosphere. The improved representation of meridional gradients demonstrates that superfluous horizontal mixing is substantially reduced with 6-h-averaged winds. Corresponding improvements are seen in the age spectrum.

4. Impacts on Ozone Assimilation

[18] While AA gives important information on the transport time through the stratosphere, it does not give complete information on the more rapidly varying aspects of the transport. One perspective on this is provided by evaluation of the sensitivity to input winds of an ozone assimilation system [*Stajner et al.*, 2001, 2004]. The diagnosis capitalizes on the availability and quality of ozone data sets and the frequent comparison between forecast and data in the assimilation.

[19] The ozone assimilation system has two components, the CTM and the assimilation modules. This version of the CTM used in this section includes a simple approximation to ozone chemistry (using production rates and loss frequencies). Two integrations of the CTM were made, unconstrained by ozone data. They were initialized in January 2000 and driven by either the snapshot or 6-h-average winds from GEOS-4, using the same time interpolation as in the AA experiments. Two corresponding ozone assimilation experiments were performed. Every 6 h, the PSAS-based assimilation module [*Stajner et al.*, 2001] blends the model forecasts with ozone retrievals from the Total Ozone Mapping Spectrometer (TOMS) [*McPeters et al.*, 1996] and the NOAA 14 Solar Backscatter Ultraviolet (SBUV) [*Bhartia et al.*, 1996] instruments.

[20] Figure 4 shows the latitudinal distributions of zonal-mean total column ozone in July 2000 from the two CTM runs and the two assimilations. The two assimilations agree

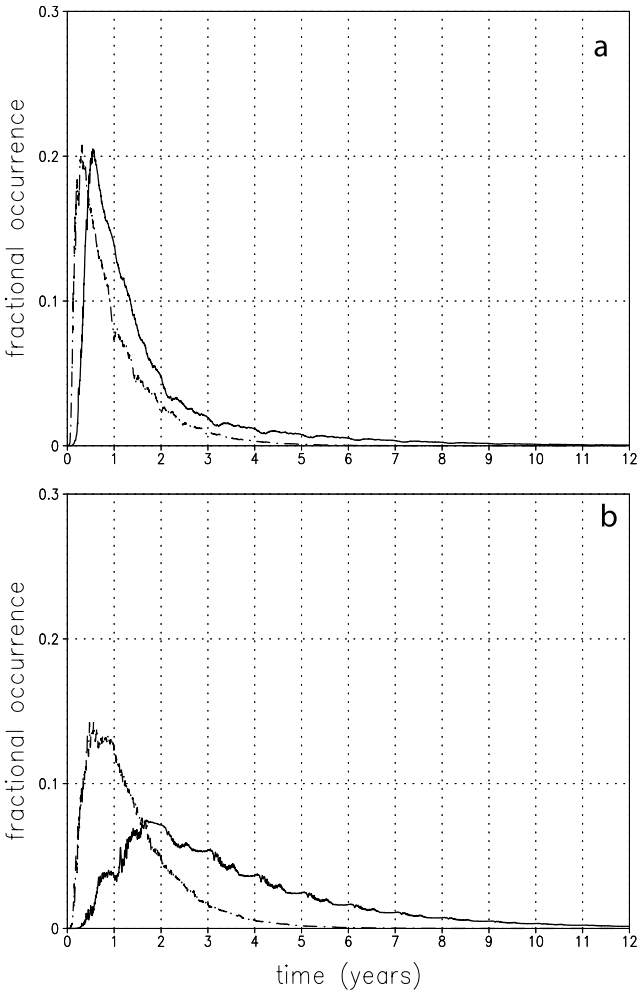

Figure 3. Probability distribution functions showing the age spectrum computed using pulse-release tracers with GEOS-4 time-averaged (solid lines) and instantaneous (dash-dotted lines) winds. Data are shown for (a) 50 hPa, 0°N, and (b) 50h Pa, 60°N.

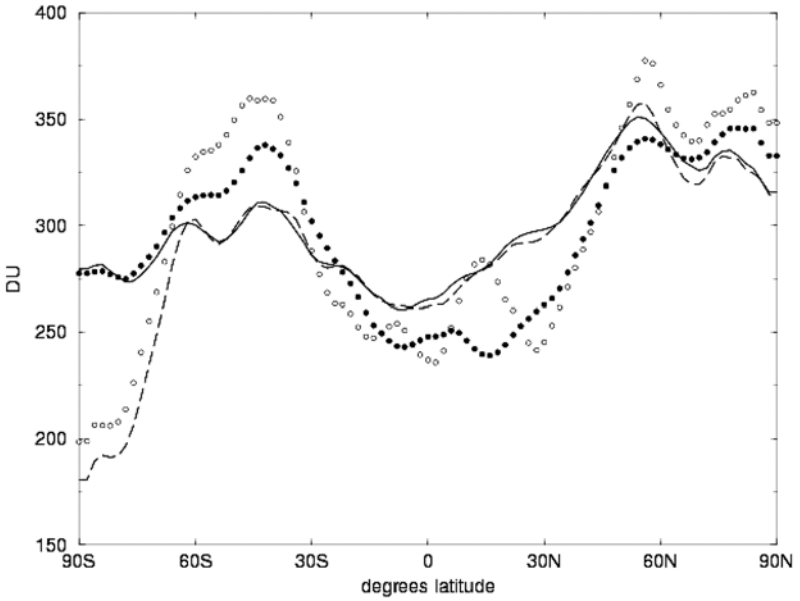

Figure 4. Total ozone (DU) in July 2000 for two simulation and two assimilation experiments using the snapshot and 6-h mean winds. Solid line shows the assimilation using 6-h-averaged winds; dashed line shows the assimilation using snapshot winds; solid circles show the simulation using 6-h-averaged winds; and open circles show the simulation using snapshot winds.

well (within 10 DU) North of about 60°S, where SBUV and TOMS data exist. Ozone in the CTM runs departs from the assimilated values, with generally a low bias in the tropics and a high bias at other latitudes, consistent with the overstrong residual circulation [*Douglass et al.*, 1997]. In the polar night, south of 63°S in July, there are no SBUV or TOMS data to assimilate. Here the curves group according to the wind data set used, with unrealistically low ozone (<200 DU) when using the snapshot winds and more reasonable values when using the 6-h averages. This effect arises from rapid mixing from tropical to polar regions seen in AA (Figure 2). The mixing diagnostic of *Tan et al.* [2004] reveals about 40% more meridional mixing into the polar night when snapshot winds are used.

[21] The vertical distribution of zonal-mean ozone concentration differences between the two assimilation runs (Figure 5) is large throughout the stratosphere in polar night. There is almost 1ppmv less ozone throughout the stratospheric vortex in the assimilation using snapshot winds: This is excessively low. *Stajner and Wargan* [2004] found that including Polar Ozone and Aerosol Measurement III data in the assimilation led to much more realistic ozone in the polar night than was possible with SBUV data. Away from the polar night, the pattern of differences in Figure 5 displays positive and negative regions, consistent with the differences in residual upwelling in the lower stratospheric region of dynamical control, where the ozone gradients are largest. To reconcile the information in Figures 4 and 5, note that the total ozone constraint in the assimilation adjusts the tropospheric partial column to compensate for differences in stratospheric ozone.

[22] Comparison with co-located ozonesonde data (Figure 6) shows that the improved transport with 6-h mean winds reduces the RMS errors by at least 20% at all levels in both the Tropics and northern middle latitudes. Similar results are obtained when validating against co-located retrievals from the Stratospheric Aerosol and Gas Experiment II [*Wang et al.*, 2002].

[23] The value of "observation minus forecast" (O-F) residuals as a tool for monitoring assimilation system performance is well established [e.g., *Hollingsworth et al.*, 1986] and has been applied to ozone assimilation. *Stajner et al.* [2004] demonstrated marked improvement in ozone O-Fs when a preliminary version of GEOS-4 winds was used in place of GEOS-3 winds in the CTM. Time series (1 April to 31 July) of the global RMS O-Fs for TOMS total ozone (Figure 7) illustrate a substantial impact of the choice of winds used in the forecast. The RMS values, which have a decreasing seasonal evolution in this period, decrease from around 17–20 Dobson Units (DU) to 9–11 DU when using 6-h-averaged in place of instantaneous winds. In the middle latitudes (not shown) there are slightly larger improvements in the southern (summer) than in the northern (winter) hemisphere. Figure 7 also includes a third ozone assimilation experiment, demonstrating that a longer (12-h) averaging period has no additional benefits. (This experiment still used four wind data sets per day, with overlapping averaging periods.)

[24] Figure 8 shows global RMS O-F fields for SBUV ozone in ten layers (Umkehr levels 3–12). In the middle and lower stratosphere (layers 3–6), where ozone chemistry is slow, there is a reduction of about one half to two thirds in the RMS of O-F when 6-h mean winds are used. Again, both the 6- and the 12-h averaging have similar impacts: The result does not support using the longer window.

[25] In summary, use of the ozone assimilation system enables quantitative measures of the impact of using different wind data sets to be made. There are substantial improvements to the quality of ozone analyses (better agreement with independent data) and to the internal statistics of the

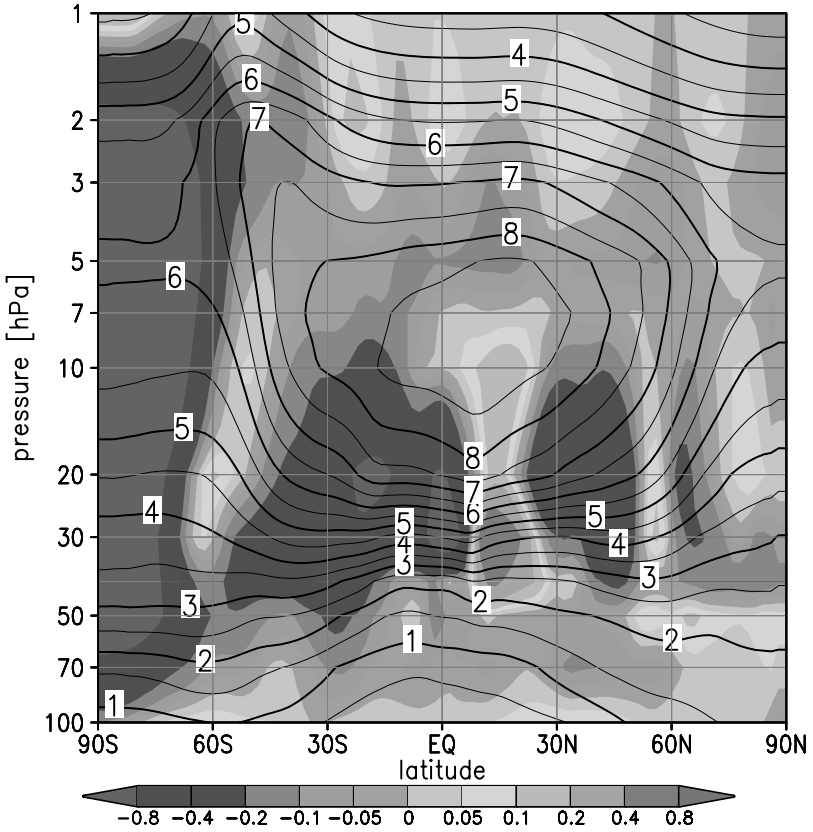

Figure 5. Zonal-mean assimilated ozone in the stratosphere (100-1 hPa) for July 2000. The contours (interval 0.5 ppmv) show the Solar Backscatter Ultraviolet + Total Ozone Mapping Spectrometer (SBUV+TOMS) assimilation using 6-h-averaged winds. The shading (interval irregular; see gray scale) shows the difference between the assimilations using instantaneous and time-mean winds (positive differences mean that instantaneous winds yield higher ozone concentrations).

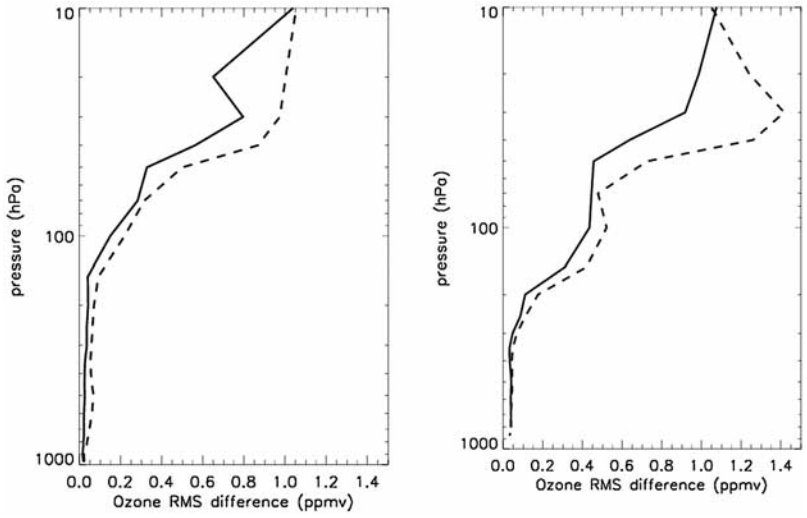

Figure 6. RMS ozone differences between assimilations and the sondes in July 2000. Values are shown for the 6-h-averaged (solid lines) and instantaneous (dashed lines) winds. (left) The tropical values are for 47 profiles in the latitude range 30°S to 30°N. (right) Northern midlatitude values are for 82 profiles in the latitude range 30°N to 60°N.

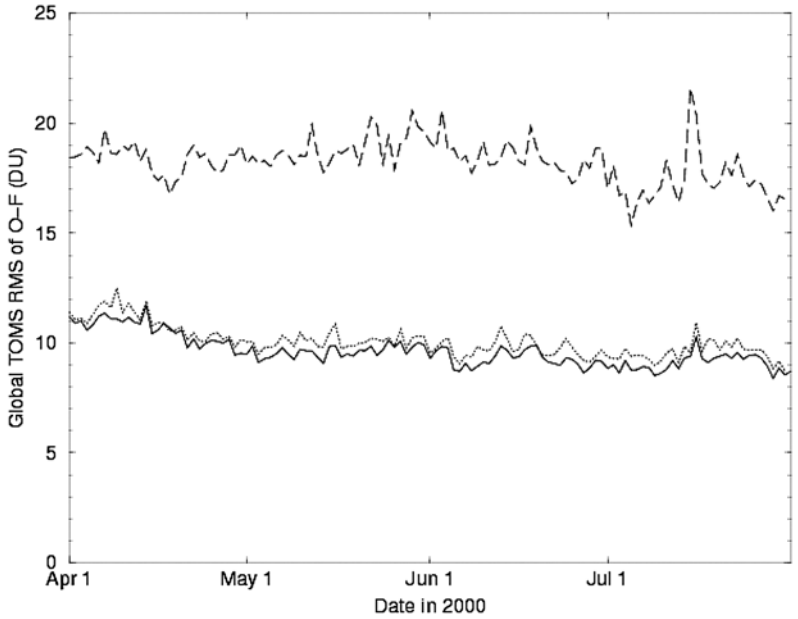

Figure 7. Time series of the global root-mean-square "observation minus forecast" (O-F) residuals in total ozone. Results are shown for the assimilations using 6-h-averaged (solid line), 12-h-averaged (dotted line), and instantaneous (dashed line) winds. The O-Fs are the departures of the chemistry-transport model (CTM) forecast from the TOMS data, aggregated at the observation locations for each day between 1 April and 31 July 2000.

system (substantial reductions in O-Fs) when 6-h average winds are used in place of snapshots.

5. Online Calculations

5.1. Motivation and Impacts

[26] Some benefits of using 6-h-averaged meteorological fields in off-line CTMs have been illustrated. The purpose of this section is to evaluate the potential of using the 6-h filtering in an on-line model, for coupled studies of meteorology and composition. This is motivated by the fact that high-frequency oscillations impact comparisons of simulated constituent fields along the flight tracks of satellite or aircraft data, as well as mixing. It is therefore desirable to eliminate the oscillation in a similar manner to the off-line CTM.

[27] *Rasch et al.* [1997] presented the MATCH technique, in which their GCM was integrated with a constraint from meteorological analyses. In this approach, the GCM fields are overwritten when analyses are available, but all subgrid

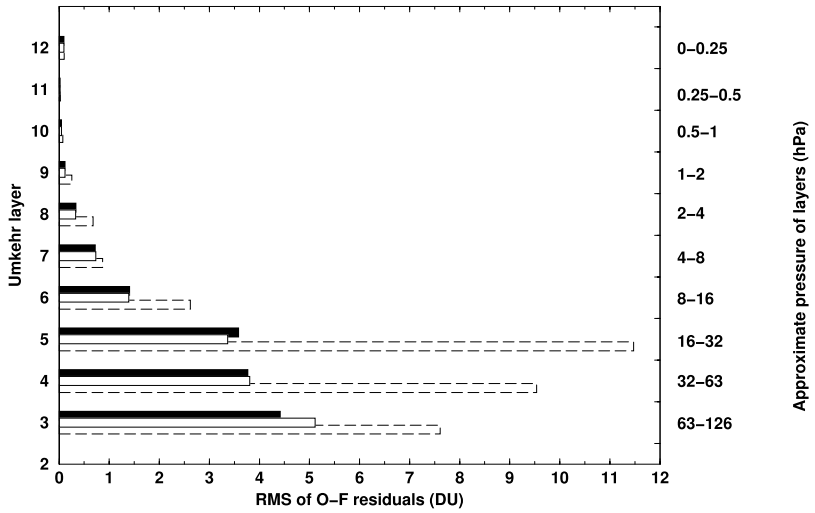

Figure 8. Global RMS of the SBUV ozone O-F residuals for the partial columns (pressure depths indicated on right-hand axis) for Umkehr layers 3–12 of the SBUV version 6 retrievals [*Bhartia et al.*, 1996] in July 2001. Results are shown for 6-h (filled) and 12-h (solid lines) time-averaged winds and for instantaneous (dashed lines) winds.

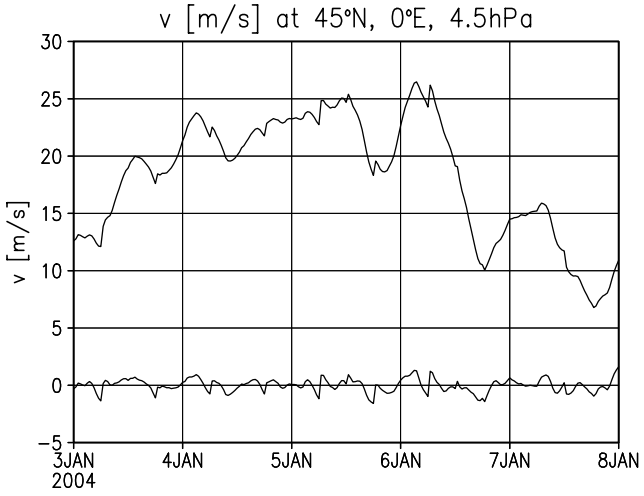

Figure 9. Time series of v (m/s) at 4.5 hPa, 0°E and 45°N, between 00Z 3 January 2004 and 00Z 8 January 2004, as in Figure 1. These curves show the raw signal and the departure from the 6-h mean computed from high-frequency output when the general circulation model (GCM) is constrained by 6-h mean fields instead of the analysis snapshots.

computations and transport are computed by the GCM at high frequency. A similar method was used in these experiments. This is similar to the concept used when making the meteorological analyses in GEOS-4: Every 6 h, the temperature, wind, moisture and surface pressure in the GCM are overwritten with the analyses (which are the instantaneous fields used in the CTM computations in sections 3 and 4). Instead of using the analyses, the 6-h-averaged meteorological fields, centered on the analysis times, can be used. This is equivalent to using the 6-h square-wave filter on the meteorological analyses. Figure 9 shows meridional winds, for the same period as shown in Figure 1, from the experiment using 6-h-averaged winds. It shows the same general behavior as in Figure 1, but with suppressed high-frequency structure.

[28] On this basis, two examples are given from on-line simulations. The first is a study of descent in the polar vortex using a stratospheric chemistry module in the GCM. The second concerns tropical water vapor. The focus here is no longer on the comparison (which does not add more information than in sections 3 and 4), but on the sustainability of long-lived features. Because of the importance of saturation in determining tropical moisture distributions, the representations of temperature minima that may occur in the GCM between the 6-hourly intervals make this a more suitable modeling framework than the off-line CTM framework.

5.2. Descent of Long-Lived Trace Gases in the Polar Vortex

[29] A number of prior studies have shown that transport in the polar region is inaccurate when assimilated winds are used. Typically, long-lived trace gases do not show realistic descent through the winter [e.g., *Considine et al.*, 2003] because of lateral mixing of midlatitude air masses across the polar vortex boundary [e.g., *Tan et al.*, 2004]. Here, polar N_2O in the GCM constrained with 6-h-averaged winds from the analyses is compared to a free-running GCM [*Stolarski et al.*, 2006] and with atmospheric observations. These results were almost identical to those in experiments using the CTM.

[30] Time-height sections of N_2O near 78°N between November and March in EOS MLS data and two simulations are shown (Figure 10). EOS-MLS retrievals of N_2O are from limb radiance measurements in the 640 GHz band [*Livesey et al.*, 2006]. Absolute accuracy is estimated as being within 20% [*Froidevaux et al.*, 2006]. The two simulations of N_2O in Figure 10 are from GEOS-4 with a chemistry model updated slightly from that of *Considine et al.* [2003], as described by *Stolarski et al.* [2006]. Spatial resolution is reduced to $2.5° \times 2°$ (longitude×latitude) at all 55 levels of the GEOS-4 GCM. The first was constrained by the 6-h mean assimilated winds in the 2004–2005 northern winter, the same period as the MLS data. The second simulation is an arbitrary year from the free-running GCM, included for reference.

[31] Figure 10 shows gradual descent of the low polar N_2O values as the season progresses; this is seen in the MLS retrievals and the two simulations. Both the MLS data and the free-running GCM simulation show the 240 ppbv contour descending through the 380K isentrope in late January, but in the 2004–2005 simulation it does not descend below 400K. This means that there is slightly too much N_2O at the lowest levels in the polar vortex, indicative of excessive lateral mixing. It is encouraging that the simulated N_2O captures the ascending contours beginning in early February, as the stratosphere is dynamically disturbed. (This feature occurs later in the free-running model because there is no temporal correspondence with disturbances in the real atmosphere.) This suggests that the behavior of long-lived constituents is reasonably well captured when 6-h averaging is applied to the winds, opening up the possibilities for study of polar chemistry and reactive gases.

5.3. Vertical Moisture Transport in the Tropical Stratosphere

[32] Figure 11 shows time series of analyzed zonal-mean temperature at 85 hPa in the Tropics for the period January 2002 until June 2004. The clear annual cycle in tropopause-region temperatures is evident in this figure, with lowest values occurring in January–March. Several studies [e.g., *Hatsushika and Yamazaki*, 2003; *Fueglistaler et al.*, 2005] have shown that the humidity in the lower stratosphere is controlled by the large-scale temperature distributions. The shaded regions in Figure 11 denote times when the saturation specific humidity at any longitude around the latitude band fell below 1.6mg/kg (approximately 2.5 ppmv) on each day. Occurrence of such values limits the specific humidity entrance values into the stratosphere. While there is a good correlation with the zonal-mean temperature, this diagnostic emphasizes some of the important longitudinal variations that serve to limit the entry values of water into the stratosphere [*Simmons et al.*, 1999]. Humidity values that enter the stratosphere are in quite good agreement with observations [e.g., *Voemel et al.*, 2002].

[33] The ascent rate of tropical water vapor concentration anomalies is examined. The so-called tape recorder signal in

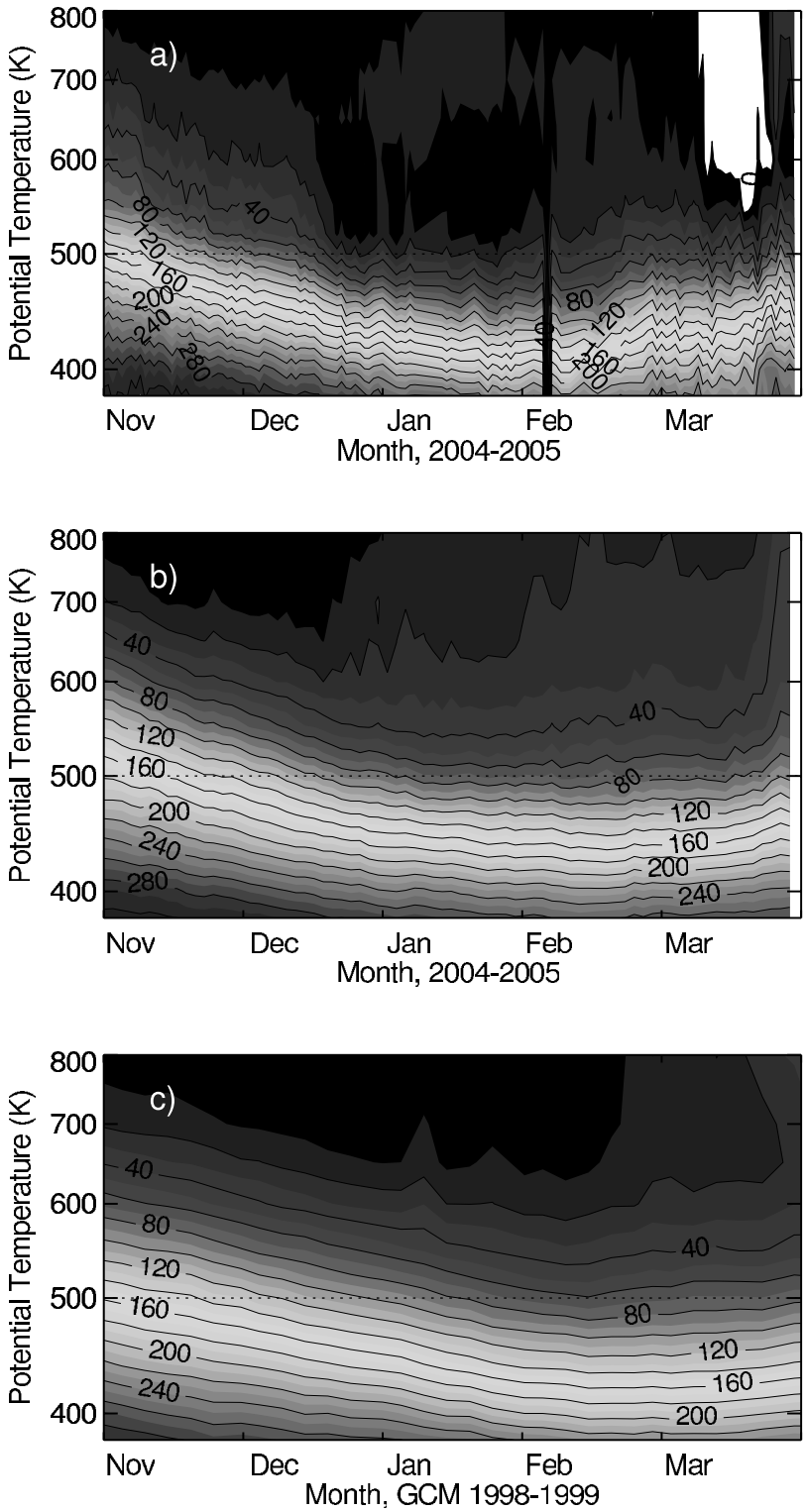

Figure 10. Time-height series of N_2O (ppbv; contour interval 20 ppbv) near 78°N on isentropic levels averaged in the polar cap (78°–90°N) for 1 November 2004 to 31 March 2005 from (a) observations (Microwave Limb Sounder retrievals), (b) the model constrained with 6-h-averaged winds, and (c) for an arbitrary year of free-running model simulation.

tropical water, isolated by *Mote et al.* [1996] in retrievals of space-based data, has become a standard diagnostic of tropical upwelling. A distinct signal is evident (Figure 12), with upward propagation of the maxima and minima in the tropical tropopause water distributions. The smallest specific humidity occurs near 85 hPa in the January–March period, consistent with the lower saturation specific humidity values, with much higher values in August–October.

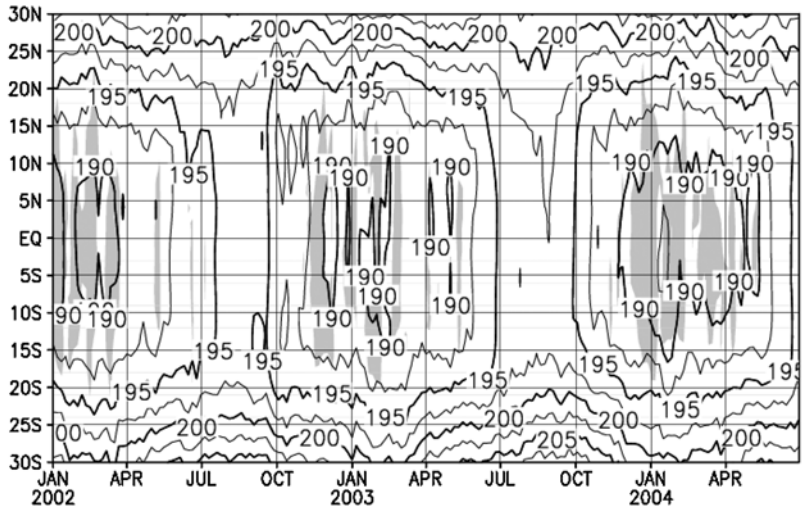

Figure 11. The zonal-mean temperature (K) at 85 hPa between 1 January 2002 and 30 June 2004. The contour interval is 2.5K. Shading indicates that the minimum saturation specific humidity around the latitude circle fell below 1.6 mg/kg (approximately 2.5 ppmv).

Throughout the year there is evidence of partial replenishment of tropical moisture just above the tropical tropopause, but the tape recorder signal propagates upward, retaining the marked annual cycle. Consistent with the AA computations, propagation speed is somewhat faster than that in observations, with ascent from 100 to 10 hPa taking about 10 months compared to 15 months in the work of *Mote et al.* [1996].

6. Conclusions and Discussion

[34] This study demonstrates that the use of 6-h-averaged winds, rather than instantaneous values with 6-h frequency, substantially improves transport calculations using winds from the GEOS-4 DAS. Application of this square-wave filter eliminates signals with periods of less than 6 h that occur in the wind data set. The averaging substantially reduces the spurious mixing that is a well-documented feature of transport computations using meteorological analyses. The results of this paper indicate that useful scientific analysis of stratospheric constituent transport can be performed using the 6-h-averaged winds.

[35] This 6-h averaging is one of several approaches that could potentially be used to improve the transport characteristics of analyzed data. Various types of filter could be applied, but the simplicity of the square wave and the fact that it is consistent with the accumulated diagnostics (e.g., cloud mass fluxes) archived by many meteorological analyses were factors in the choice. More advanced approaches would attempt to reduce the excessive transience at the source, the reconciliation of imperfect analyses with the imperfect GCM. Several approaches to this issue are being considered for GEOS-5, including initialization and reducing shocks using incremental analysis updates [*Bloom et al.*, 1996]. A potential drawback of using 6-h averages is that they potentially suppress real features, such as diurnal and semidiurnal tides. The 6-h averaging used here needs to be fully assessed in comparison with other methods, such as

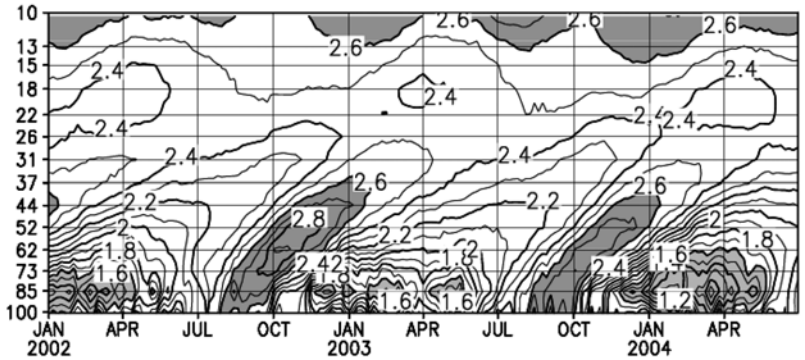

Figure 12. The water vapor tape recorder signal isolated using the 6-h averaging. The plot shows specific humidity (mg/kg) averaged in the domain bounded by 5°S and 5°N for the period 1 January 2002 through 30 June 2004. Values lower than 1.6 mg/kg (approximately 2.5 ppmv) and larger than 2.6 mg/kg are shaded to highlight these regions; the contour interval is 0.1 mg/kg. The pressure scale shows, to the nearest integer, the pressure levels of the GCM.

use of forecasts [e.g., *Wild et al.*, 2003], time-smoothed, 3-h snapshots [e.g., *Legras et al.*, 2005] or shorter averages [e.g., *Waugh et al.*, 1997].

[36] A number of validation techniques were used in this study. The suitability of the AA to illustrate the bulk nature of the stratospheric residual circulation was exploited, in the manner of prior studies [e.g., *Douglass et al.*, 2003; *Meijer et al.*, 2004]. Because such diagnostics do not allow for assessment of all aspects of stratospheric transport, other metrics were considered. The performance of an ozone assimilation system demonstrated value in assessing the more rapid aspects of transport in the lower stratosphere. Evaluation of ozone concentrations against independent data and monitoring of the system statistics (O-Fs) provided a powerful demonstration of the improved quality of the transport when using 6-h-averaged winds. Such analysis allows direct validation, which is not possible with more abstract quantities, such as mixing diagnostics [*Tan et al.*, 2004]. In the polar stratosphere, transport and mixing in and around the polar vortex was evaluated by comparing a long-lived tracer (N_2O) with values derived from atmospheric measurements. Finally, an assessment of the water distribution in the tropical lower and middle stratosphere enabled an assessment of the transport properties of the flow, showing a credible, but somewhat fast, ''tape recorder'' signal using the assimilated winds, yet noting certain inadequacies associated with excessive meridional mixing across the subtropical barrier.

[37] In summary, the 6-h averaging eliminates many of the problems associated with spurious mixing in the GEOS-4 analyses. The vigorous transport computed using analyses is calmed. The transport circulation remains too strong, as evidenced by the excessive upward propagation speed of tropical water vapor anomalies, the somewhat low AA, as well as the excess of long-lived trace gases in the low polar stratosphere. Experiments using a detailed chemistry scheme are being analyzed to assess the extent to which this overactive transport impacts long-lived trace gases and ozone chemistry in the polar vortices. Important questions remain, including the impact of this approach on analyses made with different techniques. An issue of substantial importance is the need to determine the optimal length of the averaging period, which requires a set of transport studies using instantaneous and time-averaged data constraints saved at higher frequency with shorter averaging windows than those used in this study. These will be foci for future studies. Future directions should also include fundamental research aimed at producing assimilated data sets that are in themselves viable for trace-gas transport studies.

[38] **Acknowledgments.** We thank colleagues in the Global Modeling and Assimilation Office for their constructive criticisms and input during the validation exercises that led us to adopt the time averaging as a technique for reducing the transport noise in GEOS-4. Thanks to NASA for computing resources. Comments by Bram Bregman and two anonymous reviewers helped substantially in setting the context and clarifying the presentation. S. P.'s work was partly supported by NASA grants NAG5-12162 and AURA/04-0156-0094.

References

Andrews, A. E., et al. (2001), Empirical age spectra for the midlatitude lower stratosphere from in situ observations of CO_2: Quantitative evidence for a subtropical barrier to horizontal transport, *J. Geophys. Res.*, *106*, 10,257–10,274.

Berthet, G., N. Huret, F. Lefèvre, G. Moreau, C. Robert, M. Chartier, V. Catoire, B. Barret, I. Pisso, and L. Pomathiod (2006), On the ability of chemical transport models to simulate the vertical structure of the N_2O, NO_2 and HNO_3 species in the mid-latitude stratosphere, *Atmos. Chem. Phys.*, *6*, 1599–1609.

Bhartia, P. K., R. D. McPeters, C. L. Mateer, L. E. Flynn, and C. Wellemeyer (1996), Algorithm for the estimation of vertical ozone profile from the backscattered ultraviolet (BUV) technique, *J. Geophys. Res.*, *101*, 18,793–18,806.

Bloom, S. C., L. L. Takacs, A. M. DaSilva, and D. Ledvina (1996), Data assimilation using incremental analysis updates, *Mon. Weather Rev.*, *124*, 1256–1271.

Bloom, S., et al. (2005), The Goddard Earth Observation System Data Assimilation System, GEOS DAS version 4.0.3: Documentation and validation, *NASA Tech. Memo., NASA TM-2005-104606 V26*, 166 pp.

Bregman, B., E. Meijer, and R. Scheele (2006), Key aspects of stratospheric tracer modeling using assimilated winds, *Atmos. Chem. Phys.*, *6*, 4529–4543.

Cohn, S. E., A. da Silva, J. Guo, M. Sienkiewicz, and D. Lamich (1998), Assessing the effects of data selection with the DAO Physical-Space Statistical Analysis System, *Mon. Weather Rev.*, *126*, 2913–2926.

Considine, D. B., S. R. Kawa, M. R. Schoeberl, and A. R. Douglass (2003), N_2O and NO_y observations in the 1999/2000 Arctic polar vortex: Implications for transport processes in a CTM, *J. Geophys. Res.*, *108*(D5), 4170, doi:10.1029/2002JD002525.

Douglass, A. R., R. B. Rood, S. R. Kawa, and D. J. Allen (1997), A three-dimensional simulation of the evolution of the middle latitude winter ozone in the middle stratosphere, *J. Geophys. Res.*, *102*, 19,217–19,232.

Douglass, A. R., M. R. Schoeberl, R. B. Rood, and S. Pawson (2003), Evaluation of transport in the lower tropical stratosphere in a global chemistry and transport model, *J. Geophys. Res.*, *108*(D9), 4259, doi:10.1029/2002JD002696.

Froidevaux, L., et al. (2006), Early validation analyses of atmospheric profiles from EOS MLS on the Aura Satellite, *IEEE Trans. Geosci. Remote Sens.*, *44*, 1106–1121, doi:10.1109/TGRS.2006.884366.

Fueglistaler, S., M. Bonazzola, P. H. Haynes, and T. Peter (2005), Stratospheric water vapor predicted from the Lagrangian temperature history of air entering the stratosphere in the tropics, *J. Geophys. Res.*, *110*, D08107, doi:10.1029/2004JD005516.

Hadjinicolaou, P., A. Jrrar, J. A. Pyle, and L. Bishop (2002), The dynamically driven long-term trend in stratospheric ozone over northern middle latitudes, *Q. J. R. Meteorol. Soc.*, *128*, 1393–1412.

Hall, T. M., and R. A. Plumb (1994), Age as a diagnostic of stratospheric transport, *J. Geophys. Res.*, *99*, 1059–1070.

Hatsushika, H., and K. Yamazaki (2003), Stratospheric drain over Indonesia and dehydration within the tropical tropopause layer diagnosed by air parcel trajectories, *J. Geophys. Res.*, *108*(D19), 4610, doi:10.1029/2002JD002986.

Hollingsworth, A., D. B. Shaw, P. Lonnberg, L. Illari, K. Arpe, and A. J. Simmons (1986), Monitoring of observation and analysis quality by a data assimilation system, *Mon. Weather Rev.*, *114*, 861–879.

Kiehl, J. T., J. J. Hack, G. B. Bonan, B. A. Boville, D. L. Williamson, and P. J. Rasch (1998), The National Center for Atmospheric Research Community Climate Model: CCM3, *J. Clim.*, *11*, 1131–1149.

Leblanc, T., O. P. Tripathi, I. S. McDermid, L. Froidevaux, N. J. Livesey, W. G. Read, and J. W. Waters (2006), Simultaneous lidar and EOS MLS measurements, and modeling, of a rare polar ozone filament over Mauna Loa Observatory, Hawaii, *Geophys. Res. Lett.*, *33*, L16801, doi:10.1029/2006GL026257.

Legras, B., I. Pisso, G. Berthet, and F. Lefèvre (2005), Variability of the Lagrangian turbulent diffusivity in the lower stratosphere, *Atmos. Chem. Phys.*, *4*, 1605–1622.

Lin, S.-J. (2004), A vertically Lagrangian finite-volume dynamical core for global models, *Mon. Weather Rev.*, *132*, 2293–2307.

Lin, S. J., and R. B. Rood (1996), Multidimensional flux form semi-Lagrangian transport schemes, *Mon. Weather Rev.*, *124*, 2046–2070.

Livesey, N. J., W. van Snyder, W. G. Read, and P. A. Wagner (2006), Retrieval algorithms for the EOS Microwave Limb Sounder (MLS), *IEEE Trans. Geosci. Remote Sens.*, *44*, 1144–1155, doi:10.1109/TGRS.2006.872327.

McPeters, R. D., S. M. Hollandsworth, L. E. Flynn, J. R. Herman, and C. J. Seftor (1996), Long-term ozone trends derived from the 16-year combined Nimbus 7 Meteor 3 TOMS version 7 record, *Geophys. Res. Lett.*, *23*, 3699–3702.

Meijer, E. W., B. Bregman, A. Segers, and P. F. J. van Velthofen (2004), The influence of data assimilation on the age of air calculated with a global chemistry-transport model using ECMWF wind fields, *Geophys. Res. Lett.*, *31*, L23114, doi:10.1029/2004GL021158.

Mote, P. W., K. H. Rosenlof, M. E. McIntyre, E. S. Carr, J. C. Gille, J. R. Holton, J. S. Kinnersley, H. C. Pumphrey, and J. M. Russel III (1996), An

atmospheric tape recorder: The imprint of tropical tropopause temperatures on stratospheric water vapor, *J. Geophys. Res.*, *101*, 3989–4006.
Press, W. H., S. A. Teukolsky, W. T. Vetterling, and B. P. Flannery (1992), *Numerical Recipes in Fortran: The Art of Scientific Computing*, 2nd ed., 963 pp., Cambridge Univ. Press, New York.
Rasch, P. J., N. M. Mahowald, and B. J. Eaton (1997), Representations of transport, convection, and the hydrologic cycle in chemical transport models: Implications for the modeling of short-lived and soluble species, *J. Geophys. Res.*, *102*, 28,127–28,138.
Rood, R. B., A. R. Douglass, J. A. Kaye, M. A. Geller, C. Yuechen, D. J. Allen, E. M. Larson, E. R. Nash, and J. E. Nielsen (1991), Three-dimensional simulations of wintertime ozone variability in the lower stratosphere, *J. Geophys. Res.*, *96*, 5055–5071.
Sankey, D., and T. G. Shepherd (2003), Correlations of long-lived chemical species in a middle atmosphere general circulation model, *J. Geophys. Res.*, *108*(D16), 4494, doi:10.1029/2002JD002799.
Scheele, M. P., P. C. Siegmund, and P. F. J. van Velthofen (2005), Stratospheric age of air computed with trajectories based on various 3D-Var and 4D-Var data sets, *Atmos. Chem. Phys.*, *5*, 1–7.
Schoeberl, M. R., A. R. Douglass, Z. Zhu, and S. Pawson (2003), A comparison of the lower stratospheric age spectra derived from a general circulation model and two data assimilation systems, *J. Geophys. Res.*, *108*(D3), 4113, doi:10.1029/2002JD002652.
Simmons, A. J., A. Untch, C. Jakob, P. Kallberg, and P. Unden (1999), Stratospheric water vapour and tropical tropopause temperatures in ECMWF analyses and multi-year simulations, *Q. J. R. Meteorol. Soc.*, *125*, 353–386.
Stajner, I., and K. Wargan (2004), Antarctic stratospheric ozone from the assimilation of occultation data, *Geophys. Res. Lett.*, *31*, L18108, doi:10.10.1029/2004GL020846.
Stajner, I., L. P. Riishœjgaard, and R. B. Rood (2001), The GEOS Ozone Data Assimilation System: Specification of error statistics, *Q. J. R. Meteorol. Soc.*, *127*, 1069–1094.
Stajner, I., N. Winslow, R. B. Rood, and S. Pawson (2004), Monitoring of observation errors in ozone assimilation, *J. Geophys. Res.*, *109*, D06309, doi:10.1029/2003JD004118.
Stöhl, A., O. R. Cooper, and P. James (2004), A cautionary note on the use of meteorological analysis fields for quantifying atmospheric mixing, *J. Atmos. Sci.*, *61*, 1446–1453.
Stolarski, R. S., A. R. Douglass, M. Gupta, P. A. Newman, S. Pawson, M. R. Schoeberl, and J. E. Nielsen (2006), An ozone increase in the Antarctic summer stratosphere: A dynamical response to the ozone hole, *Geophys. Res. Lett.*, *33*, L21805, doi:10.1029/2006GL026820.
Swinbank, R., R. L. Orris, and D. L. Wu (1999), Stratospheric tides and data assimilation, *J. Geophys. Res.*, *104*, 16,929–16,942.
Tan, W., M. A. Geller, S. Pawson, and A. M. da Silva (2004), A case study of excessive subtropical transport in the stratosphere of a data assimilation system, *J. Geophys. Res.*, *109*, D11102, doi:10.1029/2003JD004057.
van Noije, T. P. C., H. J. Eskes, M. van Weele, and P. F. J. van Velthoven (2004), Implications of the enhanced Brewer-Dobson circulation in ERA-40 for the stratosphere-troposphere exchange of ozone in global chemistry-transport models, *J. Geophys. Res.*, *109*, D19308, doi:10.1029/2004JD004586.
Voemel, H., et al. (2002), Balloon-borne observations of water vapor and ozone in the tropical upper troposphere and lower stratosphere, *J. Geophys. Res.*, *107*(D14), 4210, doi:10.1029/2001JD000707.
Wang, H. J., D. M. Cunnold, L. W. Thomason, J. M. Zawodny, and G. E. Bodeker (2002), Assessment of SAGE version 6.1 ozone data quality, *J. Geophys. Res.*, *107*(D23), 4691, doi:10.1029/2002JD002418.
Wargan, K., I. Stajner, S. Pawson, R. B. Rood, and W. Tan (2005), Monitoring and assimilation of ozone data from the Michelson interferometer for passive atmospheric sounding, *Q. J. R. Meteorol. Soc.*, *131*, 2713–2734.
Waugh, D. W., et al. (1997), Three-dimensional simulations of long-lived tracers using winds from MACCM2, *J. Geophys. Res.*, *102*, 21,493–21,513.
Weaver, C. J., A. R. Douglass, and R. B. Rood (1993), Thermodynamic balance of three-dimensional stratospheric winds derived from a data assimilation procedure, *J. Atmos. Sci.*, *50*, 2987–2993.
Wild, O., J. K. Sundet, M. J. Prather, I. S. A. Isaksen, H. Akimoto, E. V. Browell, and S. J. Oltmans (2003), Chemical transport model ozone simulations for spring 2001 over the western Pacific: Comparisons with TRACE-P lidar, ozonesondes, and total ozone mapping spectrometer columns, *J. Geophys. Res.*, *108*(D21), 8826, doi:10.1029/2002JD003283.

L.-P. Chang, H. Hayashi, J. E. Nielsen, S. Pawson, I. Stajner, and W.-W. Tan, Global Modeling and Assimilation Office, Code 610.1, NASA Goddard Space Flight Center, Greenbelt, MD 20771, USA. (pawson@gmao.gsfc.nasa.gov)

S. R. Kawa and Z. Zhu, Atmospheric Chemistry and Dynamics Branch, Code 613.3, NASA Goddard Space Flight Center, Greenbelt, MD 20771, USA.

N. J. Livesey, Jet Propulsion Laboratory, Pasadena, CA 91109, USA.